Int. J. Electrochem. Sci., 8 **(2013)** 5925 - 5943

International Journal of
ELECTROCHEMICAL
SCIENCE
www.electrochemsci.org

Correlation Between Inhibition Efficiency and Chemical Structure of Some Amino Acids on the Corrosion of Armco Iron in Molar HCl

A. Aouniti[1], *K.F. Khaled*[2,3,*], *B. Hammouti*[1]

[1] LCAE-UAC18, Faculté des Sciences, Université Mohammed Premier, 60000 Oujda, Morocco
[2] Electrochemistry Research Laboratory, Ain Shams University, Faculty of Education, Chemistry Department, Roxy, Cairo, Egypt
[3] Materials and Corrosion Laboratory, Taif University, Faculty of Science, Chemistry Department, Taif, Hawiya 888, Kingdom of Saudi Arabia
[*]E-mail: khaledrice2003@yahoo.com

Received: 20 October 2012 / *Accepted:* 6 February 2013 / *Published:* 1 April 2013

Weight loss measurement and various electrochemical AC and DC corrosion monitoring techniques are performed at 308 K using Armco iron specimens immersed in 1M HCl solution in the presence and absence of various amino acids (methionine, cysteine, cystine, glycine, leucine, arginine, serine, glutamic acid, ornithine, Lysine, aspartic acid, alanine, valine, asparagine, glutamine, and threonine). Polarisation curves indicated that theses amino acids act as cathodic inhibitors. Methionine, cysteine and cystine who have a sulphur atom in their molecular structure are the best inhibitors, and we suggested that theses three amino acids are adsorbed on the metal surface through the sulphur active centre and that the extent of inhibition is directly related to the formation of the adsorption layer which is sensitive function of the molecular structure. The corrosion inhibition of methionine is regarded by simple blocked fraction of the electrode surface related to the adsorption of inhibitor species according to Frumkin isotherm model on the Armco iron surface. It is clear that quantum descriptors are a better choice when predictivity is the main issue. Among the descriptors with major contribution we should point out that highest occupied molecular orbital energy (E_{HOMO}), total dipole moment, total energy and binding energy are important predictive descriptors.

Keywords: Corrosion inhibitor, Amino acids, Genetic Function Approximation, QSAR

1. INTRODUCTION

Its know that the efficiency of an organic compound as corrosion inhibitor depends not only on the characteristics of the environment in which it acts, the nature of the metal surface and electrochemical potential at the interface, but also on the structure of the inhibitor itself [1, 2] .

The inhibitor molecule should have centres capable of forming bonds with the metal surface via electron transfer. Thus, the metal acts as an electrophile, whereas the inhibitor molecule acts as a Lewis base, whose nucleophilic centre are normally available for sharing, i.e. formation of a bond.

Organic compounds containing electro-negative functional groups and π electron in triple or conjugated double bonds are usually good inhibitors [3-11].

In recent decades, the use of natural compounds, nontoxic and ecologically friendly is required in industry. In our laboratory, various researches showed that aminoacids [3-11] and some extracts or oil from natural plants [22–24] exhibited as efficient corrosion inhibitors for steel, iron and copper in different test solutions. The excellent inhibitory effect of methionine on the iron corrosion in HCl solution was patented [25].

Grigor'ev and Kusnetsov [12] studied the effect of glycine derivatives as inhibitors of the production of hydrogen in the corrosion of zinc and iron in H_2SO_4 solutions. They found that an increase in the electron acceptor properties of the substituent radical resulted in greater control of the liberation of hydrogen from the metals. Issa et al. [13] investigated the inhibiting efficiency of some amino compounds including cystine, cysteine, semicarbazide and thiosemicarbazide on the corrosion of aluminium by acids. They suggested that the adsorption of the organic compound on the metal surface took place through the C=S group in the case of thiosemicarbazide and through the C=O group in other cases. Brandt et al.[14] studied the inhibition by organic sulphides of the corrosion of iron by acids. They reported that the sulphur atom of the aliphatic sulphides is the reaction centre for their interaction with the metal surface.

Several attempts have been made to predict corrosion inhibition efficiency with a number of individual parameters obtained via various quantum chemical calculation methods as a tool for studying corrosion inhibitors [15-18] .

Khaled studied the relationship between the structural properties of several classes of organic inhibitors and their effect on their inhibition efficiencies using genetic function approximation and neural network analysis methods[1, 19, 20].

In the present work corrosion tests and electrochemical measurements are performed on Armco iron in HCl solution in the presence of some amino acids containing an active sulphur (methionine: Met, cysteine: Cys, cystine: Cyt) and a sulphur-free amino acids (glycine: Gly, leucine: Leu, arginine: Arg, serine: Ser, glutamic acid: Glu, ornithine: Orn, Lysine: Lys, aspartic acid: Asp, alanine: Ala, valine: Val, asparagine: Asn, glutamine: Gln, and threonine: Thr) to determine (a) the efficiency of these compounds as inhibitors of the corrosion of Armco iron by acid and (b) the inhibition mechanism. The structural properties of these amino acids well be calculated using quantum chemical calculations and a QSAR model will be thought.

2. EXPERIMENTAL DETAILS

All chemicals used were of AR grade and the inhibitors are from commercial products (Fig. 1). The specimens used in the chemical investigations are in the form of strips of dimensions 1cm×2cm×0.05cm. Table 1 shows the chemical composition of pure Armco iron:

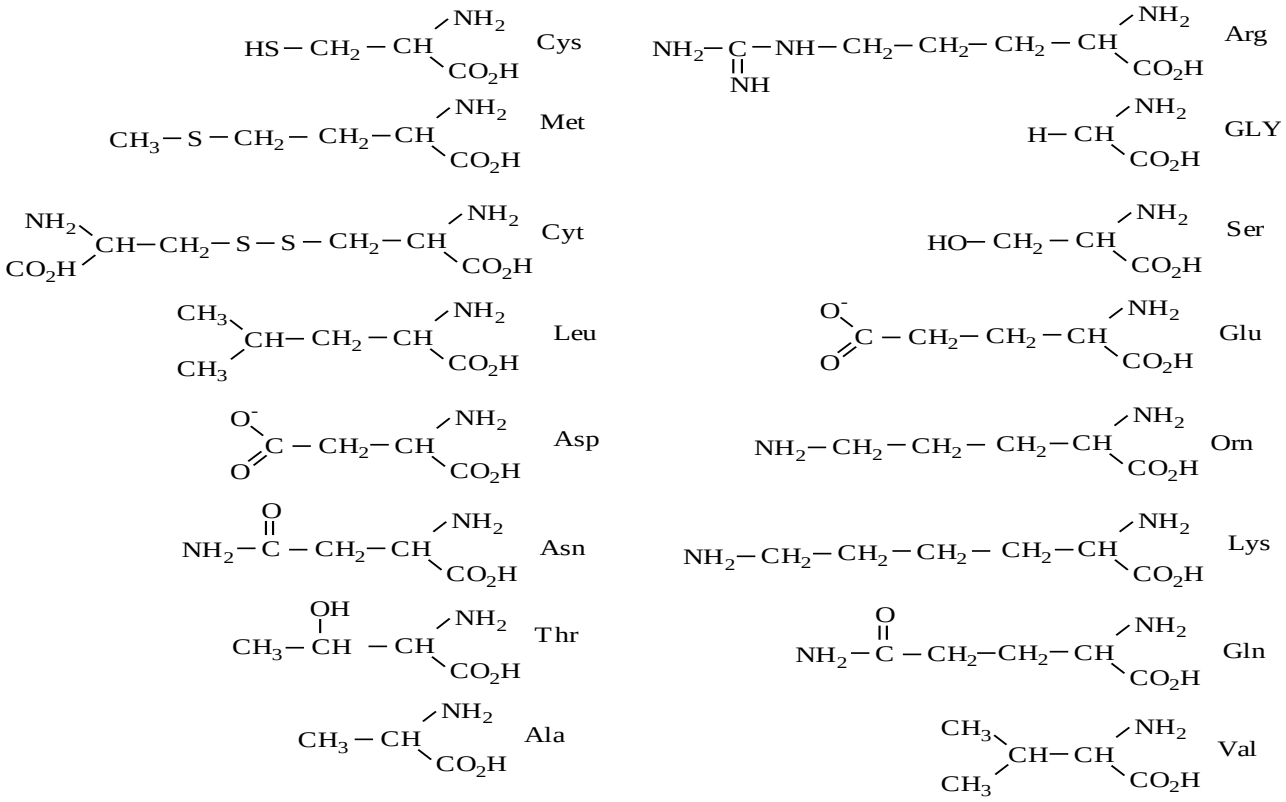

Figure 1. Molecular structure of amino acids studied.

Table 1. Chemical composition of Armco iron.

element	C	Si	Mn	S	P	Cu	Ni	Cr	N	O	Fe
%	0.012	0.01	0.07	0.006	0.008	0.025	0.02	0.015	0.042	0.072	balance

The mass loss was measured on Armco iron sheets in 100 ml of 1M HCl solution. Electrochemical impedance and potentiodynamic measurements are carried out in a conventional three-electrode electrolysis cylindrical tempered glass cell. The working electrode, in the form of a disc cut from Armco iron, had a geometric area of 1.0 cm^2. A saturated calomel electrode (SCE) and a platinum (Pt) electrode are used as reference and auxiliary electrodes, respectively. The polarisation curves are recorded with an Amel 550 potentiostat using an Amel 567 linear sweep generator at a scan rate of 20 mV/min. Before recording the cathodic polarisation curves, the iron electrode was polarised at -800 mV/SCE for 10min. For anodic curves, the potential electrode was swept from its corrosion potential maintained for 30 min, to more positive values.

All impedance spectra in the frequency range 10 mHz ≤ f ≤ 64000 Hz are performed in the potentiostatic mode at the corrosion potential, using an EGG Princeton model 6310 Frequency Response Analyser. A small amplitude signals (±10 mV) are used in the frequency domain cited. The impedance diagrams are given in the Nyquist representation (R-jG) where R is the real and -jG is the imaginary part.

The aggressive solution (1M HCl) is prepared by dilution of analytical-grade 37% HCl with doubly distilled water. All tests are obtained in magnetically stirred and deaerated solutions. Prior measurement, the iron samples are polished with different emery paper, rinsed with doubly distilled water and dried in air.

3. COMPUTATIONAL DETAILS

Geometrical parameters of all stationary points for the investigated amino acids are optimised both in gas and aqueous phases, employing analytic energy gradients. The generalised gradient approximation (GGA) within the density functional theory was conducted with the software package DMol^3 in Materials Studio of Accelrys Inc. All calculations were performed using the Becke–Lee–Yang–Parr (BLYP) exchange correlation functional and the double numerical with polarization (DNP) basis set [21-23] , since this was the best set available in DMol^3. A Fermi smearing of 0.005 hartree and a real space cutoff of 3.7 Å was chosen to improve the computational performance. All computations were performed with spin polarization.

The phenomenon of electrochemical corrosion takes place in the liquid phase, so it is relevant to include the effect of solvent in the computations. Self-consistent reaction field (SCRF) theory [24], with Tomasi's polarised continuum model (PCM) was used to perform the calculations in solution. These methods model the solvent as a continuum of uniform dielectric constant (ϵ=78.5) and define the cavity where the solute is placed as a uniform series of interlocking atomic spheres. Frontier orbital distribution was obtained, at the same basis set level, to analyse the reactivity of inhibitor molecules.

The genetic function approximation (GFA) algorithm offers a new approach to the problem of building quantitative structure-activity relationship (QSAR) and quantitative structure-property relationship (QSPR) models. Replacing regression analysis with the GFA algorithm allows the construction of models competitive with or superior to those produced by standard techniques and makes available additional information not provided by other techniques. Unlike most other analysis algorithms, GFA provides multiple models, where the populations of the models are created by evolving random initial models using a genetic algorithm. GFA can build models using not only linear polynomials but also higher-order polynomials, splines, and other nonlinear functions [25].

4. RESULTS AND DISCUSSION

4.1 Comparative experimental studies.

The structure of the amino acids tested are shown in Fig. 1. The effect of addition of amino acids on the corrosion of iron in 1M HCl solution was also studied by weight-loss at 308K after 6 hours of immersion period (Table 2). Inhibition efficiency (E_w%) are calculated as follows:

$$E_w\,\% = (1 - \frac{w}{w^o}) \times\ 100$$

where w and w^o are the corrosion rates of iron samples in the absence and presence of the organic compounds, respectively.

The cathodic and anodic polarisation curves of iron in molar HCl in the absence and presence of these molecules at 10^{-3}M are presented in Figs. 2 and 3, respectively.

The curves reveal that all amino acids tested at 10^{-3}M inhibit only the cathodic process and Met, Cys and Cyt who have a sulphur atom in their structure are the best inhibitors. The organic compounds studied perform their inhibiting action by slowing down the cathodic reaction of hydrogen. Values of associated electrochemical parameters and inhibition efficiency ($E_{pot}\%$) of all compounds are given in Table 2. In this case of polarisation method, no Tafelic straight line was found especially with Met, Cys, Cyt and Arg, then the inhibition efficiency ($E_{pot}\%$) is determined by the relation:

$$E_{pot}\% = 1 - \frac{i_{corr}}{i^o_{corr}} \times 100$$

Where $i_{corr} = i_{corr} / A$: A is the exposed surface area and i^o_{corr}, i_{corr} are the uninhibited and inhibited corrosion current densities, respectively, for a given ($E_{pot}\%$)

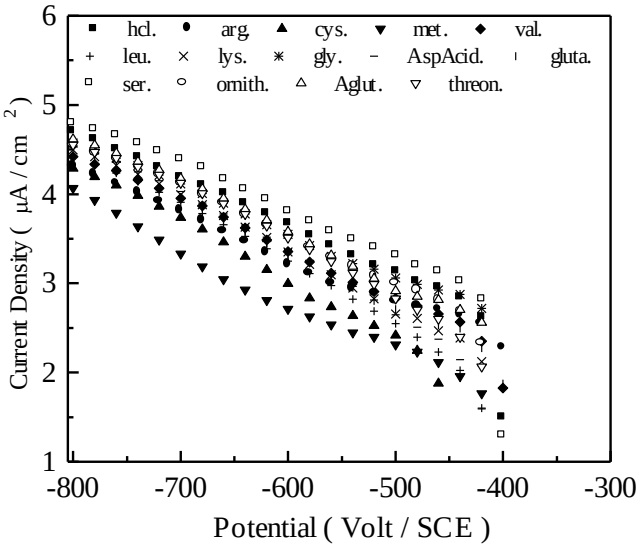

Figure 2. Cathodic potentiokenitic polarisation curves of Armco iron in 1M HCl in the presence of different amino acids.

The inhibiting properties of many compounds are determined by electron density at the atom containing the main reaction centre [26]. In our work, all inhibitors discussed have an acidic and amine functions in their structure. Further, owing to the acidity of the medium, amino acid compounds cannot remain in solution as free molecules and they exist in the solution in the cationic form:

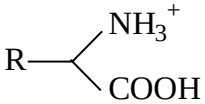

"R" is a radical

However, variation in inhibition efficiency among the various additives would originate from the changing nature of substituents in the end of the radical « R ».

Table 2. Gravimetric and electrochemical data of the iron corrosion in 1M HCl with various amino acids at 10^{-3}M.

compounds	HCl	Met	Cys	Cyt	Arg	Val	Leu	Lys	Gly	Asp	Gln	Ser	Orn	Glu	Thr	Ala	Asn
Gravimetric measurements																	
W(mg.cm^{-2}.h^{-1})	0.572	0.156	0.239	0.225	0.189	0.482	0.240	0.364	0.563	0.489	0.492	0.579	0.430	0.530	0.418	0.506	0.418
E %	---	72.7	58.2	60.7	66.9	15.7	58.0	36.4	1.6	14.5	14.0	-1.2	24.8	7.3	26.9	11.5	26.9
Polarisation measurements																	
E_{corr} (mV)	-477	-485	-497	-488	-472	-464	-466	-478	-460	-468	-460	-483	-475	-466	-474	-461	-463
E = -700 mV																	
I (µA/cm^2)	15100	2140	5400	4090	6430	9000	8060	9820	13000	10740	9280	24400	12900	14900	13300	9560	7440
E %	- - -	85.8	64.2	72.9	57.4	40.4	46.6	35.0	13.9	28.9	38.5	-61.6	14.6	1.3	11.9	36.7	50.7
E = -600 mV																	
I (µA/cm^2)	4540	515	980	1180	1620	2270	1780	2239	3539	2390	2060	6470	3310	3780	3230	2090	2238
E %	- - -	88.7	78.4	74.0	64.3	50.0	60.8	50.7	22.0	47.4	54.6	-42.5	27.1	16.7	28.8	54.0	50.7
E = -500 mV																	
I (µA/cm^2)	1332	205	260	248	627	676	353	452	1153	442	514	2000	973	818	673	732	355
E %	- - -	84.6	80.4	81.4	52.9	49.2	73.5	66.1	13.4	66.8	61.4	-50.1	26.9	38.6	49.5	45.0	73.3

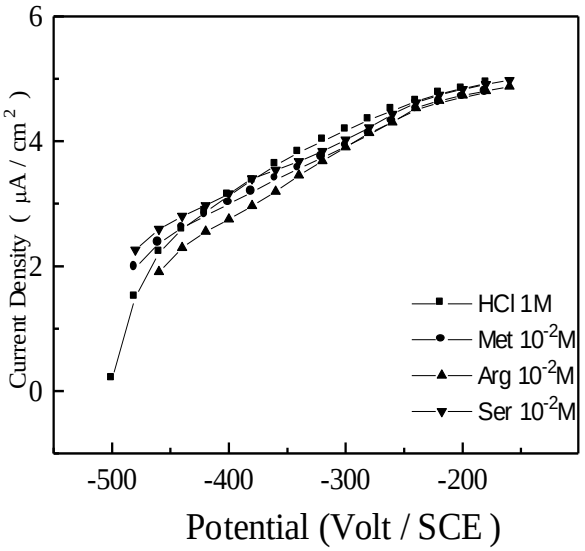

Figure 3. Anodic potentiokenitic polarisation curves of Armco iron in 1M HCl in the presence of some amino acids.

Electron donating substituents, would be expected to enhance adsorption and subsequent corrosion inhibition to a degree dependent on the magnitude of electron charge density on the active centre. The insertion of radicals improved the inhibiting effect as follows (gravimetric results in Table 2):

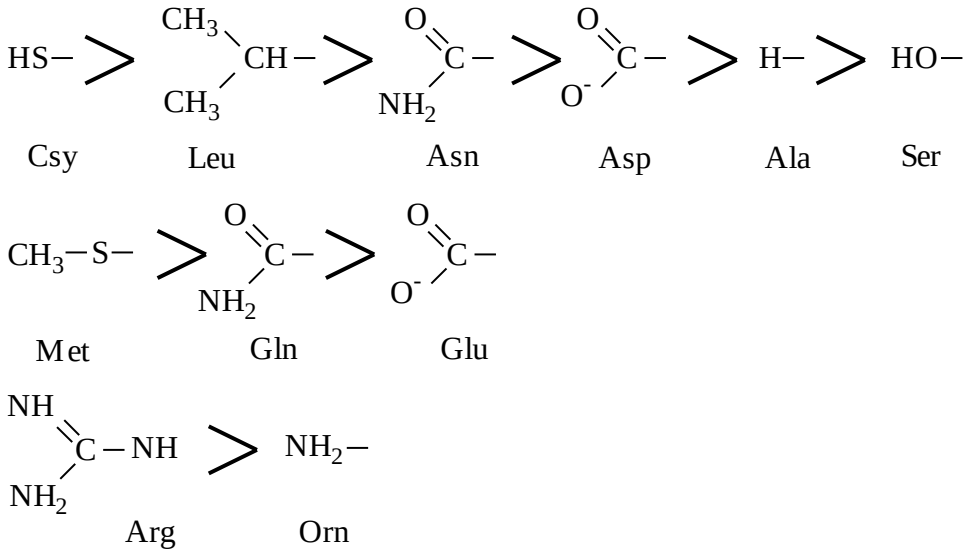

The inhibiting efficiency of the compounds depends on many factors which include the number of adsorption actives centres in the molecule and their charge density, molecule size, mode of adsorption and formation of metalic copmlex [26-28].

The essential effect of the corrosion inhibition is due to presence of electron donors groups (N, O, S) in the molecular structure of amino acid tested. The presence of free electron pairs in the nitrogen, sulphur atoms and π electron on double bond favours the adsorption of the inhibitor.

Comparison of the experimental data given in Table 2 indicates that the inhibition efficiency of compounds Ala, Leu, Asp, Asn and Lys is greater than that Gly, Val, Orn, Glu and Gln, respectively. This behaviour is explained on the basis on the difference in the number of the carbon atoms in the chaine of radical « R ». The inhibition efficiency changes with increasing number of CH_2 group in radical « R » of the molecule.

We have two cases:

1°) If the substituent at the end of the radical « R » is an electron donating substituent, then inhibition efficiency increase with increasing number of CH_2 group in radical « R » of the molecule.

Ala > Gly ; Leu > Val ; Lys > Orn

2°) On the other hand, if the substituent is an acceptor substituent, then inhibition efficiency decrease with increasing number of CH_2 group in radical « R » of the molecule.

Asp > Glu ; Asn > Gln

The addition of Ser to blank solutions increased the cathodic and anodic current densities without shifting the corrosion potential. The negative E% values indicated that this compound stimulated the corrosion process. This result indicated Ser had a catalytic effect on the proton discharge and on iron dissolution.

Brandt et al [14]. reported that the sulphur atom is the active centre of the aliphatic sulphides in their interaction with the metal surface. Therefore cysteine, cystine and methionine are adsorbed at the metal surface through the sulphur active centre. To confirm this argument the effect of a sulphur-free amino acid (alanine) on the corrosion of Armco iron in acid was studied.

Figure 4 shows the change in the degree of surface coverage θ as a function of the logarithm of the concentration of Cys and Ala. Cys shows a stronger inhibiting effect than Ala. These results

indicate that the presence of the sulphur atom in the amino acid leads to an increase in its inhibition efficiency and also causes a drastic change in its adsorption mechanism. Accordingly, one can safety conclude that the additives are adsorbed on the surface through sulphur atoms.

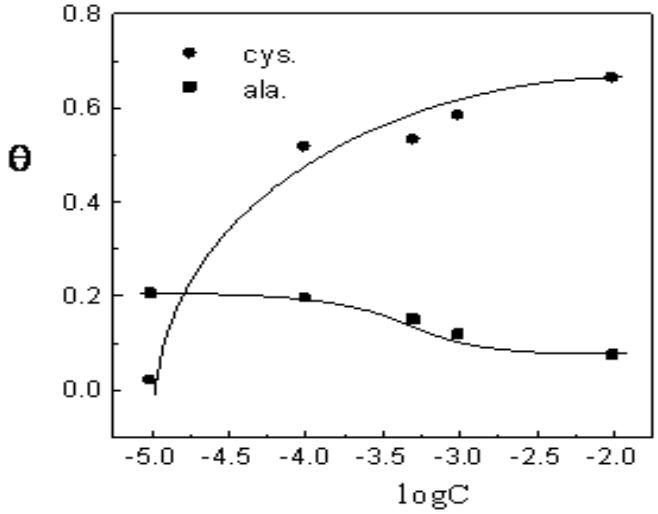

Figure 4. The dependence of the degree of coverage of the Armco iron surface with cysteine and alanine on their concentration in 1M HCl.

It appears that inhibition efficiency at 10^{-3}M of these three sulphur-containing amino acids increase in the order:

Met > Cyt > Cys

This order can be explained on the basis of the regular dependance of the inhibition efficiency on the molecular structure. Contrary to B.A. Abd-El-Naby [29], the large volume of the thioether (Cyt, Met) offers a good stability and performance to the adsorbed layer at the metal-solution interface.

Theses results confirm the previous suggestion that the amino acids are adsorbed on the metal surface through the sulphur active centre and that the extent of inhibition is directly related to the formation of the adsorption layer which is sensitive function of the molecular structure. The similar inhibition effect on the cathodic lines of three sulphur-containing amino acids can be attributed to the preferential orientation of the molecules at the metal-solution interface with the positively charged $-NH_3^+$ group which is present in all the compounds used. It was concluded that Met was the best inhibitor among the amino acids tested, and the detailed study then was conducted.

4.1.1 Detailed study of Met

Table 3 collects the values of corrosion rates of iron and inhibition efficiency of Met studied at various concentrations. According to this table, it is clear that for Met, the iron corrosion rate values decrease when the concentration increases. The inhibiting action is more pronounced with 10^{-2}M (82.5 %).

Table 3. Gravimetric and electrochemical data of the iron corrosion in 1M HCl at different concentrations of Met.

Concentration	HCl 1M	10^{-2}M	10^{-3}M	5.10^{-4}M	10^{-4}M	10^{-5}M	10^{-6}M
Gravimetric measurements							
W(mg.cm^{-2}.h^{-1})	0.572	0.1	0.156	0.186	0.237	0.366	0.378
E %	---	82.5	72.7	67.5	58.6	36.0	33.9
Polarisation measurements							
E_{corr} (mV)	-477	-488	-485	-490	-484	-487	-485
E = -700 mV							
I (µA/cm^2)	15100	1362	2140	2290	4770	8800	8660
E %	---	91.0	85.8	84.8	68.4	41.7	42.6
E = -600 mV							
I (µA/cm^2)	4540	423	515	546	1320	2940	2951
E %	---	90.7	88.7	88.0	70.9	35.2	35.0
E = -500 mV							
I (µA/cm^2)	1332	220	205	240	670	1000	1000
E %	---	83.5	84.6	82.0	49.7	24.9	24.9

The curves in Figure 5 reveal that Met inhibit only the cathodic process, and its effectiveness increases with the increased concentration in solution.

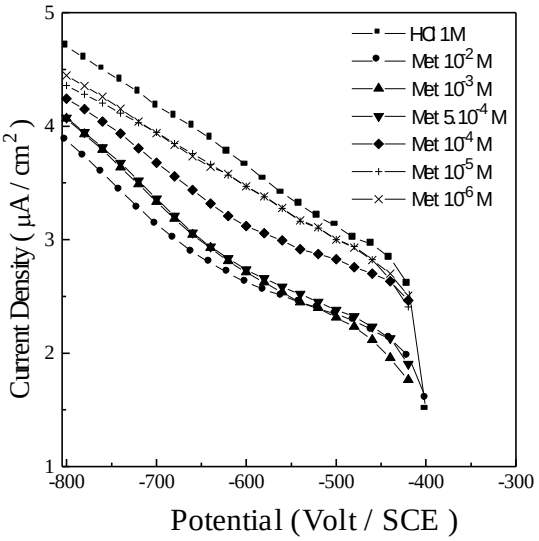

Figure 5. Cathodic potentiokenitic polarisation curves of Armco iron in 1M HCl in the presence of different concentrations of Met.

4.1.1.1 Effect of temperature:

Temperature can affected the iron corrosion in the acidic media in the absence and presence of inhibitor. To determine the activation energy of the corrosion process, gravimetric measurements are

taken at various temperatures (308-353K) in the absence and presence of Met at 10^{-2}M. The corresponding results are given in Table 4.

Although the weight-loss due to the corrosion increases with temperature, the inhibition efficiency of Met was found to increase slightly with the rise in temperature from 308 to 333K (82.5 % → 84.8 %) and above 333K, the efficiency decrease and search 73.9% at 353K.

Figure 6 shows Arrhenius plots for iron corrosion. The apparent activation energies in the absence (E_a) and presence (E'_a) of Met can be determined by the relation:

$W = K.\exp(-E_a/RT)$ $W' = K.\exp(-E'_a/RT)$

E_a = 83.4 kJ /mol E'_a = 84.2 kJ /mol

We note the stabilities of the apparent activation energy in the presence of Met.

Table 4. Influence of temperature on the corrosion rate of Armco iron electrode immersed in 1M HCl and in 1M HCl + 10^{-2}M of Met.

Temperature (K)	Corrosion rate in 1M HCl (mg.cm^{-2}.h^{-1})	Corrosion rate in 1M HCl + 10^{-2}M of Met (mg.cm^{-2}.h^{-1})	Inhibition efficiency E%
308	0.572	0.100	82.5
313	0.900	0.128	85.8
323	2.031	0.294	85.5
333	4.704	0.714	84.8
343	12.975	3.653	71.8
353	34.576	9.037	73.9

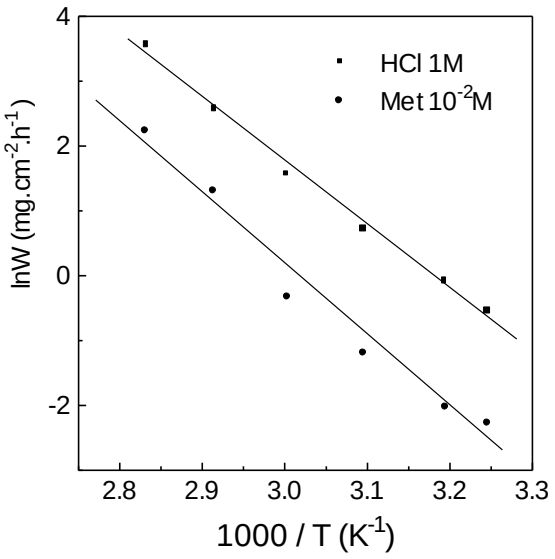

Figure 6. Arrhenius plots calculated from corrosion rate in 1M HCl and in 1M HCl + 10^{-2}M of Met.

4.2 EIS measurements.

The EIS experiments give similar results (figure 7 and Table 5). The complex spectra exhibit three less-than-half circles for three different concentrations of Met at E_{corr}. The impedance plots extrapolate at high frequencies to almost zero value for the solution resistance Rs between the Armco iron electrode and the reference electrode.

An iron electrode dissolving in the active state in acid media shows impedance diagrams similar to a semicircle in Nyquist plot [30-33], which corresponds to an electrochemical charge transfer process. In our tests, in hydrochloric acid solution, the impedance diagram does not show perfect semicircle and the imaginary part of the faradic impedance is zero even at very low frequency values. This difference has been attributed to the frequency dispersion.

According to Frignani et al. [34, 35], in the presence of very corrosion efficient derivatives the capacitive loop deviates from a semicircle, while in the presence of not very corrosion efficient additives, the impedance diagram is rather similar to a perfect semicircle. In no case is a clear inductive loop found, as happens in the presence of other types of organic additives [36-38]. In EIS measurements, the inhibition efficiencies $E_{EIS}\,\%$ are calculated as follow:

$$E_{EIS}\,\% = (1 - \frac{R_t^{'}}{R_t}) \times\ 100$$

R_t and $R_t^{'}$ are the charge transfer resistance in absence and in presence of Met, respectively. The values of the capacity associated with the different loop are calculated from the relation:

$C_{dl} = 1/\ 2\pi f_o\ R_t$

where R_t represents the diameters of different loops and f_o is the frequency at R_t /2.

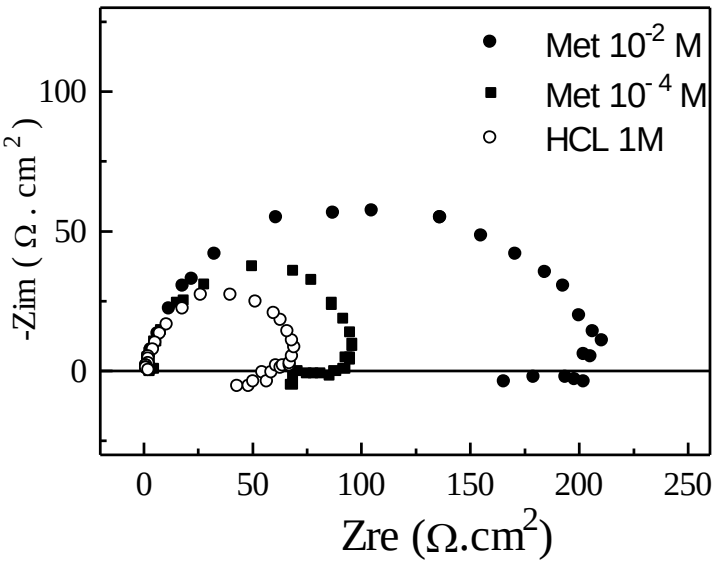

Figure 7. Electrochemical galvanostatic impedance diagrams of the Armco iron electrode in 1M HCl with various concentration of Met.

Table 5. Impedance parameters for the corrosion of Armco iron in 1M HCl in the absence and in presence of different concentrations of Met.

Concentration (M)	R_t ($\Omega.cm^2$)	f_o (Hz)	C_{dl} ($\mu F/cm^2$)	E%
0 M	68	40	58	-
10^{-2} M	228	15.0	46.5	70.1
10^{-4} M	105	40.4	37.5	35.2

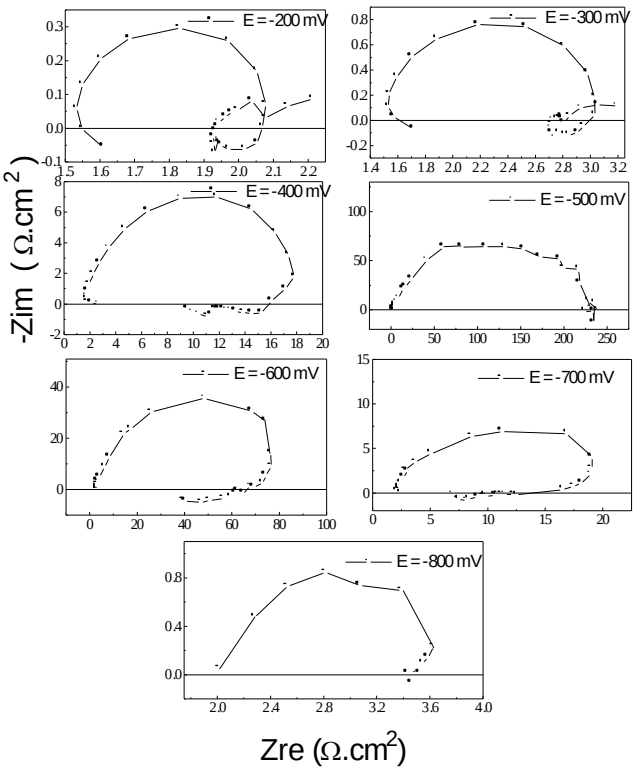

Figure 8. Electrochemical galvanostaic impedance diagrams of the Armco iron electrode in 1M HCl at various potantials.

It is observed from Table 5 that the value of R_t increases with the increase in the concentration of the inhibitor at E_{corr}. As impedance diagrams for solution examined have almost a semicircular appearance, it indicates that the corrosion of Armco iron is mainly controlled by charge transfer process. In fact, the presence of Met enhances the value of R_t in acidic solution. Values of double layer capacitance are also brought down to the maximum extent in the presence of Met and the decrease in the values of C_{dl} follows the order similar to that obtained for values of I_{Ei} in this study. The decrease in C_{dl} may be due to the adsorption of inhibitor on the metal surface leading to the formation of a film from acidic solution, similar results were also observed [50] for the case of adsorption of inhibitor or especially for polymer coated metals, C_{dl} can become so small.

For all potentials (Figs. 8 and 9) the impedance diagrams present well defined capacitive loops at high frequencies. Moreover, low frequencies inductive loops appear at anodic potentials proving an active dissolution of the metal.

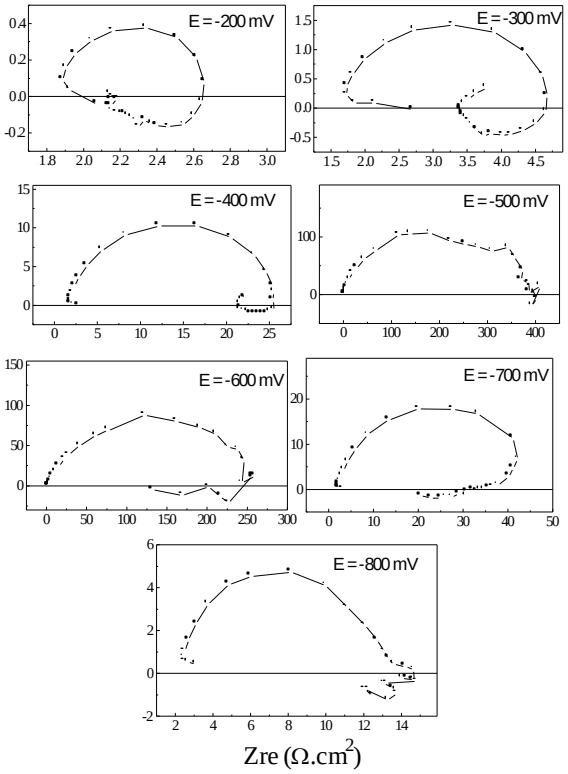

Figure 9. Electrochemical galvanostaic impedance diagrams of the Armco iron electrode in 1M HCl + 10^{-2}M of Met at various potantials.

Table 6. Electrochemical parameters of iron in 1M HCl without and with addition of Met given by polarisation and EIS measurements at different potentials. Corresponding corrosion inhibition efficiencies.

E (mV)	-800	-700	-600	-500	-400	-300	-200
Polarisation measurements							
I (μA/ cm^2) HCl only	50118	15100	4540	1332	1321	14870	69600
I (μA/cm^2) HCl + Met 10^{-2} M	7500	1362	423	220	995	8190	50200
E %	85.0	91.0	90.7	83.5	24.7	44.9	27.9
EIS measurements							
R_t (Ω.cm^2) HCl only	1.73	20	86	251.8	17.95	1.65	0.6
R'_t (Ω.cm^2) HCl + Met 10^{-2} M	12.3	54	270	470	26	3.3	0.83
E %	85.9	63.0	68.1	46.4	31.0	50.0	27.7

It is clear that AC impedance results depend on the potentials amplitude and showing the non-linearity of the system under study which is due to the discontinuity of the adsorption isotherm of the amino acid at the desorption potential as demonstrated in figure 3. In this case, the corrosion rate in the presence of Met can only be estimated at higher frequencies, diminishing both metal dissolution and inhibitor desorption process (Table 6).

Nevertheless, the Tables 2-6 show that in the presence of various concentrations of Met no evident differences are found in the inhibiting efficiency values obtained with the different methods.

The fraction of the surface covered by adsorbed molecules of the inhibitor (θ) was determined by the ratio E%/100. The relation E% and logC, where C is the amino acid concentration, had the character of an S-shaped adsorbed isotherm (figure 10). This result showed that Met was adsorbed on the iron surface electrode according to the Frumkin isotherm:

$\theta\ (1-\theta)^{-1}\exp(-f.C) = K.C.$

where K is the equilibrium constant of the adsorption reaction, f is a function of adsorption energy, and θ is the surface coverage.

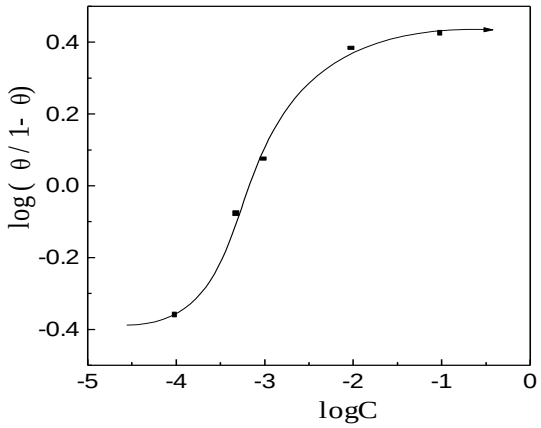

Figure 10. Frumkin isotherm adsorption model of Met on the surface of Armco iron in 1M HCl solution

Chemisorption plays an important role in the action mechanism of this additive. In point of fact higher inhibiting efficiency values are experienced by increasing not only the surface coverage of the amino acid, but also by increasing their π electrons availability.

Moreover, a likely relationship is obtained between chemisorption and the deviation of the capacitive loop from a perfect semicircle [36].

4.3 QSAR study

To understand the quantitative structure and activity relationships of the studied class of amino acids and their inhibition efficiencies on iron corrosion in 1.0 M HCl, a statistical analysis using genetic function approximation (GFA) method has been performed. A study table was belt and presented in Table 7. Second, a correlation matrix, Table 8 was derived, and then regression parameters were obtained. Table 7 shows the structural descriptors for the training set (the class of the amino acids used in this study). It includes include total energy, HOMO , LUMO, energy gap (LUMO-HOMO) and binding energy between the amino acid and the iron surface.

A univariate analysis is performed on the inhibition efficiency data in Table 9 as a tool to assess the quality of the data available and its suitability for next statistical analysis. Data in Table 9

show acceptable normal distribution. Statistical parameters presented in Table 9 have been discussed in details in our previous study [20].

Table 8 contains a correlation matrix which gives the correlation coefficients between each pair of columns included in the analysis in Table 7. Correlation coefficients between a pair of columns approaching +1.0 or -1.0 suggest that the two columns of data are not independent of each other. The cells in the correlation matrix, Table 8 are colored according to the correlation value of in each cell. Inspection of Table 8 shows that the descriptors most highly correlated with corrosion inhibition efficiency include: LUMO energy , total dipole moment, total energy, binding energy and energy gap of the inhibitor molecule. After constructing the correlation matrix the genetic function approximation algorithm will be used to perform a regression analysis. The GFA algorithm works with a set of strings, called a population. This population is evolved in a manner that leads it toward the objective of the search. Following this, three operations are performed iteratively in succession: selection, crossover, and mutation. Newly added members are scored according to a fitness criterion. In the GFA, the scoring criteria for models are all related to the quality of the regression fit to the data. The selection probabilities must be re-evaluated each time a new member is added to the population [39].The procedure continues for a user-specified number of generations, unless convergence occurs in the interim. Convergence is triggered by lack of progress in the highest and average scores of the population.

Table 10 shows the GFA analysis which gives summary of the input parameters used for the calculation. Also, it reports whether the GFA algorithm converged in specified number of generations. The GFA algorithm is assumed to have converged when no improvement is seen in the score of the population over a significant length of time, either that of the best model in each population or the average of all the models in each population. When this criterion has been satisfied, no further generations are calculated.

Table 7. Descriptors for the studied amino acids inhibitor molecules calculated using quantum chemical methods

Experimental corrosion inhibition	HOMO eigenvalue (VAMP Electrostatics)	LUMO eigenvalue (VAMP Electrostatics)	Total dipole (VAMP Electrostatics)	Total energy (DMol3 Molecular)	Binding energy (DMol3 Molecular)	HOMO energy (DMol3 Molecular)	LUMO energy (DMol3 Molecular)	LUMO-HOMO energy (DMol3 Molecular)
11.5	-10.3589	-0.40431	4.199	-321.111	-2.19048	-0.20824	-0.12033	0.087908
66.9	-8.37501	-0.43918	6.944	-601.475	-4.41508	-0.16743	-0.11647	0.05096
26.9	-9.98429	-0.5164	3.329	-488.491	-2.9702	-0.1911	-0.11844	0.072663
14.5	-10.3697	-0.84148	1.942	-508.265	-2.8307	-0.1902	-0.12584	0.064359
58.2	-8.9818	-0.76803	1.772	-717.964	-2.29689	-0.19374	-0.1298	0.063947
60.7	-8.46022	-2.33617	4.296	-1.43E+03	-4.40306	-0.17321	-0.13414	3.91E-02
7.3	-10.6179	-0.67916	7.863	-547.194	-3.33906	-0.21803	-0.13424	0.083789
14	-9.91646	-0.45563	8.049	-527.421	-3.47946	-0.19654	-0.12097	0.075566
1.6	-10.6003	-0.56603	2.125	-282.168	-1.66767	-0.20397	-0.11707	0.086905
18	-10.3111	-0.31439	3.576	-437.962	-3.77893	-0.20718	-0.11253	0.094649
36.4	-9.86675	-0.36782	2.956	-492.87	-4.07566	-0.1845	-0.11386	0.070636
72.7	-8.63782	-0.39101	5.459	-795.864	-3.35085	-0.18227	-0.12079	0.061477
24.8	-9.92098	-0.33094	2.661	-453.924	-3.55101	-0.19024	-0.11376	0.076473
27.2	-10.2768	-0.51608	2.597	-395.822	-2.37681	-0.20643	-0.12397	0.082461
16.9	-10.4808	-0.33151	5.453	-434.763	-2.89764	-0.20207	-0.11552	0.086548
15.7	-10.2822	-0.40849	4.061	-399.006	-3.24319	-0.20708	-0.12169	0.085388

Table 8. Correlation matrix of the studied variables

	B : Experimental corrosion inhibition	C : HOMO eigenvalue (VAMP Electrostatics)	D : LUMO eigenvalue (VAMP Electrostatics)	E : Total dipole (VAMP Electrostatics)	F : Dipole x (VAMP Electrostatics)	G : Dipole y (VAMP Electrostatics)	H : Dipole z (VAMP Electrostatics)	I : Total energy (DMol3 Molecular)	J : Binding energy (DMol3 Molecular)	K : HOMO energy (DMol3 Molecular)	L : LUMO energy (DMol3 Molecular)	M : LUMO-HOMO energy (DMol3 Molecular)
B : Experimental corrosion inhibition	1	0.959224	-0.33007	0.056595	0.36345	0.04030	-0.13438	-0.68855	-0.46897	0.795299	-0.16369	-0.80469
C : HOMO eigenvalue (VAMP Electrostatics)	0.959224	1	-0.43546	0.158705	0.45057	-0.01502	-0.14252	-0.75411	-0.52601	0.847113	-0.20463	-0.87098
D : LUMO eigenvalue (VAMP Electrostatics)	-0.33007	-0.43546	1	0.061089	-0.84595	-0.49305	0.13484	0.862683	0.26598	-0.37814	0.695097	0.665249
E : Total dipole (VAMP Electrostatics)	0.056595	0.158705	0.061089	1	-0.19992	-0.76763	0.77447	-0.13971	-0.43847	0.007689	-0.13694	-0.06976
F : Dipole x (VAMP Electrostatics)	0.363459	0.450572	-0.84595	-0.19992	1	0.40081	-0.29435	-0.69455	-0.23956	0.505598	-0.58183	-0.73033
G : Dipole y (VAMP Electrostatics)	0.040308	-0.01502	-0.49305	-7.68E-01	0.40081	1	-0.51099	-2.6E-01	0.232437	0.116928	-0.23521	-0.21499
H : Dipole z (VAMP Electrostatics)	-0.13438	-0.14252	0.134849	0.774473	-0.29435	-0.51099	1	0.043906	-0.06923	-0.3439	-0.32748	0.165592
I : Total energy (DMol3 Molecular)	-0.68855	-0.75411	0.862683	-0.13971	-0.69455	-0.26219	0.04390	1	0.526216	-0.6093	0.579513	0.824427
J : Binding energy (DMol3 Molecular)	-0.46897	-0.52601	0.26598	-0.43847	-0.23956	0.232437	-0.06923	0.526216	1	-0.58877	-0.05774	0.513792
K : HOMO energy (DMol3 Molecular)	0.795299	0.847113	-0.37814	0.007689	0.50559	0.11692	-0.3439	-0.6093	-0.58877	1	0.061384	-0.88945
L : LUMO energy (DMol3 Molecular)	-0.16369	-0.20463	0.695097	-0.13694	-0.58183	-0.23521	-0.32748	0.579513	-0.05774	0.061384	1	0.401573
M : LUMO-HOMO energy (DMol3 Molecular)	-0.80469	-0.87098	0.665249	-0.06976	-0.73033	-0.21499	0.16559	0.824427	0.513792	-0.88945	0.401573	1

Table 9. Univariate analysis of the inhibition data

	B : Experimental corrosion inhibition
Number of sample points	16
Range	73.9
Maximum	72.7
Minimum	-1.2
Mean	30.93125
Median	25.85
Variance	569.891
Standard deviation	24.6553
Mean absolute deviation	20.9141
Skewness	0.391719
Kurtosis	-1.4668

Table 10. Validation Table of the Genetic Function Approximation

	Predicted Inhibition Efficiency = 32.5 (HOMO) - 1.3 (Total dipole) + 0.002 (Total energy) - 0.686 (Binding energy) + 225.36 (LUMO-HOMO)
Friedman LOF	251.01264400
R-squared	0.93587300
Adjusted R-squared	0.90380900
Cross validated R-squared	0.70908200
Significant Regression	Yes
Significance-of-regression F-value	29.18803100
Critical SOR F-value (95%)	3.34514500

The Friedman's lack-of-fit (LOF) score in Table 10 evaluates the QSAR model. The lower the LOF, the less likely it is that GFA model will fit the data. The significant regression is given by F-test, and the higher the value, the better the model.

Figure 11 shows the relationship between the measured corrosion inhibition efficiencies of the studied inhibitors presented in Table 6 and the predicted efficiencies calculated by the following equation:

Predicted Inhibition Efficiency = 32.5 (HOMO) - 1.3 (Total dipole)
+ 0.002 (Total energy) - 0.686 (Binding energy)
+ 225.36 (LUMO-HOMO)

The distribution of the residual values against the measured corrosion inhibition efficiencies values are presented in Fig. 11. The residual values can be defined as the difference between the predicted value generated by the model and the measured values of corrosion inhibition efficiencies.

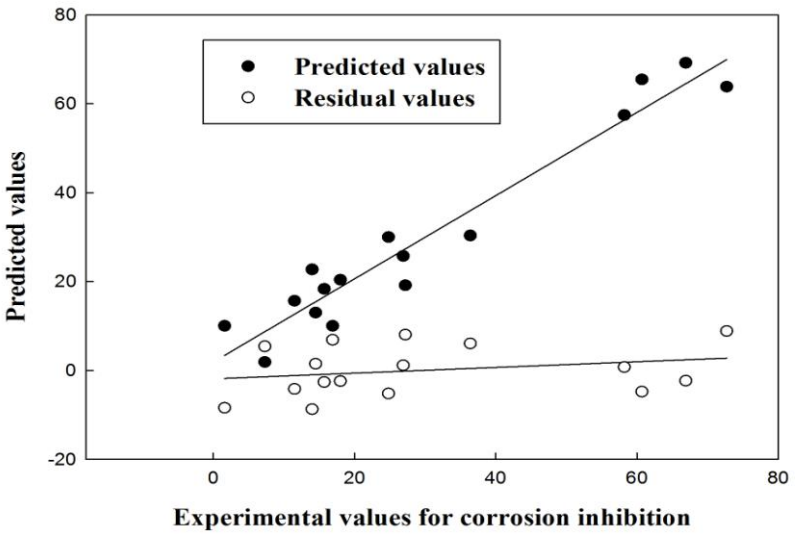

Figure 11. Plot of predicted inhibition and residuals versus measured corrosion inhibition

5. CONCLUSION

Steady-state electrochemical measurements have shown that all amino acids tested act as cathodic inhibitors. Met, Cys and Cyt who have a sulphur atom in their molecular structure are the best inhibitors and they are adsorbed at the metal surface through the sulphur active centre. Met was the best inhibitor in the serie tested and its inhibition efficiency increases with its concentration . The corrosion inhibition by methionine is interpreted by assuming that it simply blocked a fraction of the electrode surface where the adsorption of inhibitor species take place according to a Frumkin isotherm model on the iron surface. Inhibition efficiency was found to increase slightly with the rise in temperature from 308 to 333K. The computational method has proved satisfactory for the inhibition efficiency estimations. High correlation was obtained with the multivariate correlation, i.e. all the indices combined together, where the prediction power was very high for GFA. Although GFA proved to be efficient in predicting ability, more work is still required toward understanding structure-property correlation on inhibition corrosion studies, particularly concerning the analysis of different structural chemical descriptors.

References

1. K. Khaled, N. Abdel-Shafi, N. Al-Mobarak, *Int. J. Electrochem. Sci*, 7 (2012) 1027-1044.
2. O.L. Riggs, J.K. Morrison, D.A. Brunsel, *Corrosion*, 35 (1976) 356.
3. D. Eaves, G. Williams, H.N. McMurray, *Electrochim. Acta*, 79 (2012) 1-7.
4. D. Kesavan, M.M. Tamizh, M. Gopiraman, N. Sulochana, R. Karvembu, *J Surfactants Deterg*, 15 (2012) 567-576.
5. A. Sudheer, M.A. Quraishi, E.E. Ebenso, M. Natesan, *Int. J. Electrochem. Sci*, 7 (2012) 7463-7475.
6. J. Jose Santana, M. Paehler, W. Schuhmann, R.M. Souto, *Chempluschem*, 77 (2012) 707-712.
7. A. Aytac, S. Bilgic, G. Gece, N. Ancin, S.G. Oztas, *Mater Corros*, 63 (2012) 729-734.
8. G.-h. Chen, J.-m. Zhao, *Chem Res Chinese U*, 28 (2012) 691-695.
9. A. Chetouani, K. Medjahed, S.S. Al-Deyab, B. Hammouti, I. Warad, A. Mansri, A. Aouniti, *Int. J. Electrochem. Sci*, 7 (2012) 6025-6043.
10. A.S. Fouda, M. Abdallah, I.S. Ahmed, M. Eissa, *Arab. J. Chem.*, 5 (2012) 297-307.
11. B.M. Mistry, N.S. Patel, S. Sahoo, S. Jauhari, *Bull. Mater. Sci.*, 35 (2012) 459-469.
12. V.P. Grigor'ev, V.V. Kuznetsov, I. Vyssh, U. Zaved, *Khim. Khim. Tekhnol*, 11 (1968) 1237.
13. I.M. Issa, A.A. El-Samahy, Y.M. Temerk, *J. Chem. U.A.R.*, 13 (1970) 121.
14. H. Brandt, M. Fischer, K. Schwab, *Corros. Sci.*, 10 (1970) 631.
15. M. Ozcan, F. Karadag, I. Dehri, *Colloid Surf.A*, 316 (2008) 55-61.
16. G. Bereket, C. Ogretir, C. Ozsahin, *J Mol Struc-Theochem*, 663 (2003) 39-46.
17. Q. Zhao, Y. Liu, E.W. Abel, *Appl. Surf. Sci.*, 240 (2005) 441-451.
18. C. Öğretir, B. Mihçi, G. Bereket, *J Mol Struc-Theochem*, 488 (1999) 223-231.
19. K. Khaled, N. Al-Mobarak, *Int. J. Electrochem. Sci*, 7 (2012) 1045-1059.
20. K.F. Khaled, *Corros. Sci.*, 53 (2011) 3457-3465.
21. J.R. Mohallem, T. de O. Coura, L.G. Diniz, G. de Castro, D. Assafrão, T. Heine, *J. Phys. Chem. A*, 112 (2008) 8896-8901.
22. J.A. Ciezak, S.F. Trevino, *J. Phys. Chem. A*, 110 (2006) 5149-5155.
23. J. Zhang, G. Qiao, S. Hu, Y. Yan, Z. Ren, L. Yu, *Corros. Sci.*, 53 (2011) 147-152.
24. M.W. Wong, M.J. Frisch, K.B. Wiberg, *J. Am. Chem. Soc.*, 113 (1991) 4776-4782.
25. K. Khaled, N. Abdel-Shafi, *Int. J. Electrochem. Sci*, 6 (2011) 4077-4094.

26. A. Aouniti, B. Hammouti, M. Brighli, S. Kertit, F. Berhili, S. El-Kadiri, A. Ramdani., *J. Chim. Phy*, 93 (1996) 1262.
27. A.S. Fouda, M.N. Moussa, F.I. Taha, A.I. Elneanaa, *Corros. Sci.*, 26 (1986) 719-726.
28. N.A.F. Al-Rawashdeh, A.K. Maayta, *Anti-Corros Method M.*, 52 (2005) 160-166.
29. B.A. Abd-El-Nabey, N. Khalil, A. Mohamed, *Surface Technology*, 24 (1985) 383-389.
30. S.S.A. El-Rehim, M.A.M. Ibrahim, K.F. Khaled, *J. Appl. Electrochem.*, 29 (1999) 593-599.
31. K.F. Khaled, *Electrochim. Acta*, 48 (2003) 2493-2503.
32. K. Khaled, N. Hackerman, *Electrochim. Acta*, 48 (2003) 2715-2723.
33. K. Khaled, N. Hackerman, *Mater. Chem. Phys.*, 82 (2003) 949-960.
34. A. Frignani, M. Tassinari, C. Monticelli, G. Trabanelli, *Corros. Sci.*, 27 (1987) 75-81.
35. A. Frignani, C. Monticelli, G. Brunoro, G. Trabanelli, Proc. Proceeding of 6th European Symposium on Corrosion Inhibitors, Ann, Univ, Ferrara,, 1985.
36. W.J. Lorenz, F. Mansfeld, *Corros. Sci.*, 21 (1981) 647-672.
37. I. Epelboin, M. Keddam, *Electrochim. Acta*, 17 (1972) 177-186.
38. I. Epelboin, C. Gabrielli, M. Keddam, *Corros. Sci.*, 15 (1975) 155-171.
39. Accelrys Materials Studio 6.0 Manual, (2011).